Defect and Diffusion Forum Vols. 297-301 (2010) pp 838-843
Online available since 2010/Apr/13 at www.scientific.net

doi:10.4028/www.scientific.net/DDF.297-301.838

Theoretical Investigation of the Relation Between the Output of a Methane Internal Reforming SOFC and the Composition of the Feedstream

E. Vakouftsi[a], C. Athanasiou[b], G. Marnellos[a,b], F.A. Coutelieris[c]

[a]Department of Mechanical Engineering, University of Western Macedonia, Greece,
[b]Chemical Process Engineering Research Institute, Centre for Research & Technology, Greece
[c]Department of Environmental & Natural Resources Management, University of Ioannina, Greece

evakouftsi@uowm.gr, marnel@cperi.certh.gr, fkoutel@cc.uoi.gr

Keywords: SOFC, transport processes, methane, internal steam reforming, modeling.

Abstract. It is a common point for the current fuel cell research to correlate the composition of the feedstream to the output of a Solid Oxide Fuel Cell (SOFC). In this direction, the detailed steady-state transport processes (i.e. the flow regime, the heat transfer, the mass and the charge transport) are mathematically described here. A new mesoscopic mathematical model has been developed through the relative differential equations along with the appropriate boundary conditions, which have been numerically integrated by using the commercially available software CFD-ACE+, in order to calculate the electricity produced by the fuel cell. It is found that the produced current density increases with CH_4 percentage in the feeding mixture.

Nomenclature

$[A/V]_{eff}$	effective surface to volume ratio of the catalyst
b_{PR} , b_R	stoichiometric coefficients of the products and reactants
$[C_i]$	near wall molar concentration of the i reacting species, given as $[C_i] = \rho \frac{Y_i}{M_i}$
$[C_{i,ref}]$	molar concentration at a reference state at inlet
emf	open circuit voltage
h	total enthalpy of the fluid
h_i	enthalpy of the i species
$\underline{i}$	current density vector
i_e	index for electrochemical reactions
$\underline{i_F}$, $\underline{i_S}$	current density vector flowing through the pores (ionic phase) and the solid parts of the porous medium (electronic phase)
j_0	exchange current density
$\underline{J_i}$	the species i mass diffusion flux, which is calculated by the Fick's law
j_T	current flux, given as $-\nabla \cdot \underline{i_F} = \nabla \cdot \underline{i_S} = j_T$ [1]
k	thermal conductivity of the mixture

k_{eff}	effective thermal conductivity of the mixture, given as $k_{eff} = -2k_S + \frac{1}{\frac{\varepsilon}{2k_S + k_F} + \frac{1-\varepsilon}{3k_S}}$ [2]
k_F , k_S	thermal conductivity of the fluid and of the solid parts of the porous medium
M_i	molar weight of the i species
N	total number of reacting species
N_g	total number of gas species in the system
P	pressure
$\dot{Q}$	additional thermal sources due to exothermic/endothermic reactions
t	time
$\underline{U}$	velocity vector
Y_i	mass fractions of the i chemical species
$Y_{P,i}$	mass fraction of the i species in the pore fluid
V_c	cell voltage
a_a , a_c	anodic and cathodic charge transfer coefficients
a_k	concentration exponent
δ	diffusion length scale
ε	porosity of the medium
η	overpotential, given as $\eta = \varphi_S - \varphi_F$
κ	permeability of the porous material
μ	viscosity of the fluid
ρ	fluid density
σ_F , σ_S	ionic and solid phase conductivity
$\bar{\tau}$	shear stress tensor
φ_F , φ_S	ionic potential of the fluid and electric potential of the solid
$\dot{\omega}_i$	production/destruction rate of the i chemical species due to reactions, given as $\dot{\omega} = \rho D_i \frac{Y_i - Y_{P,i}}{\delta} [A/V]_{eff}$ for surface reactions and as $\dot{\omega} = (b_{PR} - b_R)\frac{j_T}{F}$ for electrochemical reactions [3]

Introduction

Fuel cells are electrochemical devices that directly convert the chemical energy of gaseous fuels into electricity without Carnot limitations, thus reaching significantly high efficiencies. Among other fuel cell types, Solid Oxide Fuel Cells (SOFC) present considerable advantages due to their high operating temperature, which favor electrochemical reaction kinetics, permitting the use of low cost metal catalysts, while they allow external or even internal reforming reactions to occur. Thus, fuels such as carbon monoxide and hydrocarbons (the first considered as poison to low temperature fuel cells), can be used with minimal fuel processing presenting not only wide feedstock flexibility, but also the opportunity to operate with naturally found and easily stored and transported fuels, such as natural gas (up to 95% CH_4) [4].

In general, most of the research correlates the efficiency of the fuel cell with the macroscopic operational parameters, based on the first and second laws of thermodynamics [5]. The main

drawback of such approaches is that the transport processes occurred in micro- and meso-scaling level are not usually taken into consideration, although they have been proved to be very important for the power production in fuel cells of any type [6]. As a first step to this direction, the main objective of this work is to identify the dependence of the current density on the CH_4 concentration in the feedstream, by taking into account the transport processes occurred.

Electrochemical and Surface Reactions

Besides hydrogen, methane/steam mixtures can be quite attractive feedstock for SOFCs. To this end, in the current study methane/steam mixtures were directly supplied in a SOFC anode and reformed to H_2 and CO through the catalytic internal steam reforming reaction as follows [7,8]

$$CH_4 + H_2O \leftrightarrow CO + 3H_2 \quad (1)$$

while the water gas shift reaction (WGS),

$$CO + H_2O \leftrightarrow CO_2 + H_2 \quad (2)$$

was considered in rapid equilibrium.

Regarding electrochemistry, the most commonly used electrodes of Ni/YSZ catalyze the electro-oxidation of both H_2 and CO [7,9]. In the present work, the electrochemical oxidation of both H_2 and CO is considered, on contrary to the majority of SOFC simulation works where the contribution of CO is neglected [8]. The relative reactions can be described as:

$$H_2 + O^{2-} \rightarrow H_2O + 2e^- \quad (3)$$

$$CO + O^{2-} \rightarrow CO_2 + 2e^- \quad (4)$$

Transport Phenomena

For the three dimensional model developed herein, the fundamental transport phenomena occurring are the flow, the heat transfer and the mass transport, as well as the charge transfer, which are described by the continuity, momentum and species (neutral or charged) conservation equations. Therefore, the velocity field, the temperature profile, the gas composition and the electric potential distribution in the fuel cell can be calculated. For a better insight of the involved processes, the fuel cell geometry can be divided in two general regions: one is the non porous region, which refers to the gas channels and the second includes the porous parts of the fuel cell i.e. the anode and the cathode electrodes, the electrolyte and the current collectors. A two dimensional cut of the fuel cell is depicted in Figure 1, where the dimensions have been chosen in accordance with Ramakrishna et al. [10].

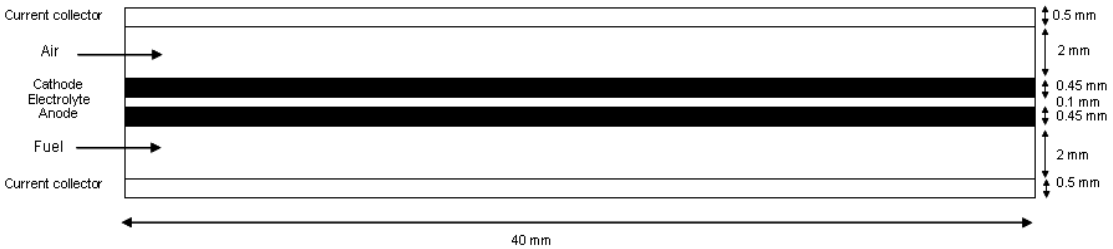

Figure 1: Simulated SOFC geometry.

The transport processes taken into account are described by the equations summarized in Table 1. Porous materials are involved in SOFC configurations, as mentioned previously, thus the transport equations of the gas phase have to be slightly modified to incorporate the porous nature of the electrodes and simulate the transport processes there.

Transport in gas phase

Process	Equation
mass conservation	$\frac{\partial \rho}{\partial t} + \nabla \cdot (\rho \underline{U}) = 0$
Flow	$\frac{\partial}{\partial t}(\rho \underline{U}) + \nabla \cdot (\rho \underline{U}\underline{U}) = -\nabla P + \nabla \cdot \bar{\tau}$
heat (energy) transfer	$\frac{\partial}{\partial t}(\rho h) + \nabla \cdot (\rho \underline{U} h) = \nabla \cdot (k \nabla T) + \frac{\partial P}{\partial t} + \dot{Q}$
mass transport	$\frac{\partial}{\partial t}(\rho Y_i) + \nabla \cdot (\rho \underline{U} Y_i) = \nabla \cdot \underline{J_i} + \omega_i$

Transport in porous medium

Process	Equation
mass conservation	$\frac{\partial}{\partial t}(\varepsilon \rho) + \nabla \cdot (\varepsilon \rho \underline{U}) = 0$
flow	$\frac{\partial}{\partial t}(\varepsilon \rho \underline{U}) + \nabla \cdot (\varepsilon \rho \underline{U}\underline{U}) = -\varepsilon \nabla P + \nabla \cdot (\varepsilon \bar{\tau}) + \frac{\varepsilon^2 \mu}{\kappa} \underline{U}$
heat (energy) transfer	$\frac{\partial}{\partial t}(\varepsilon \rho h) + \nabla \cdot (\varepsilon \rho \underline{U} h) = \nabla \cdot \left(k_{eff} \nabla T + \sum_{i=1}^{N_g} \underline{J_i} h_i \right) + \varepsilon \bar{\tau} \nabla \underline{U} + \varepsilon \frac{dP}{dt} - j_T \eta + \frac{\lvert \underline{i} \rvert^2}{\sigma}$
mass transport	$\frac{\partial}{\partial t}(\varepsilon \rho Y_i) + \nabla \cdot (\varepsilon \rho \underline{U} Y_i) = \nabla \cdot \underline{J_i} + \omega_i$

Charge transport

Process	Equation
charge conservation	$\nabla \cdot \underline{i} = 0$
transfer current in the conducting materials	$\nabla \cdot (\sigma_F \nabla \varphi_F) = -\nabla \cdot (\sigma_S \nabla \varphi_S) = j_T$
transfer current in the non-conducting electrolyte	$\nabla \cdot (\sigma_F \nabla \varphi_F) + \nabla \cdot (\sigma_S \nabla \varphi_S) = 0$
charge transfer	$j_T = \frac{j_0}{\prod_{i=1}^{N} [C_{i,ref}]^{a_{ie}}} \left[\exp\left(\frac{a_a F}{RT} \eta \right) - \exp\left(-\frac{a_c F}{RT} \eta \right) \right] \prod_{i=1}^{N} [C_i]^{a_{ie}}$

Table 1: Mathematical formulation of the transport problem in a typical SOFC.

Simulations

The numerical solution for the equations previously described was obtained by using the commercial package CFD-ACE+ by ESI-Group©, which is based on the finite volume method, in order to achieve residual values for all the quantities less than 10^{-4}. The three dimensional fuel cell was discretized in space by a structured grid consisting of 33516 cells.

To achieve the solution, the assumptions made are described below

- *Flow*: laminar conditions for compressible fluids, no gravitational effects, Darcy's law for porous regions
- *Heat transfer*: no radiation
- *Mass transport*: no accumulation
- *Charge transfer*: Ohm's law, Butler-Volmer equation
- *Feedstream*: methane/steam mixture of several compositions (25-40 % mol CH_4 and 75-60 % mol H_2O). It should be outlined that the carbon to steam ratio was kept above two in order to prevent carbon formation on the electrodes.
- *Atmospheric air:* typical composition (21 % mol O_2 and 79 % mol N_2).

Regarding the applied boundary conditions, the mass flow rates for the anodic and the cathodic mixtures were assumed to be equal to 2.4 $x10^{-6}$ mol/s and 2.0 $x10^{-5}$ mol/s for anode and cathode, respectively, while pressure was set to 1 atm at the inlets and the outlets. Preheated mixtures at 1073 K entered the fuel cell, while heat flux was set zero at all the rest of the boundaries (adiabatic operation), while zero mass flux was set at the walls and at the outlets as well. Finally, a constant value of zero potential was set to the anode collector, while the potential of the cathode collector was set to several discrete values.

Results and Discussion

The effect of the inlet composition on the gas species molar fractions was examined by studying the spatial distribution of the involving gas species along a line in the middle of the fuel cell anode channel for constant cell voltage (= 0.5 V). To begin with, Figure 2 depicts the behavior of CH_4 and H_2O for four different inlet compositions, where it is rather obvious that lower methane percentages correspond to faster consumptions, which are quite higher near the entrance of the fuel cell due to the methane steam reforming reaction. On the contrary, the electrochemical reactions imply steam production even close to the outlet of the anode. This allegation can be further verified in Figure 3, where the molar fractions of H_2 and CO are presented. Their consumption rate is higher than their production rate near the outlet, while enriched CH_4 mixtures lead to higher H_2 and CO production, as expected. The O_2 molar fraction distribution along a line in the middle of the fuel cell cathode channel is depicted in Figure 4. In accordance with H_2 and CO, O_2 is gradually consumed due to the electrochemical reactions, and as expected, the decrease in its molar fraction is maximized neat the exit. Additionally, higher CH_4 compositions correspond to increased O_2 consumption.

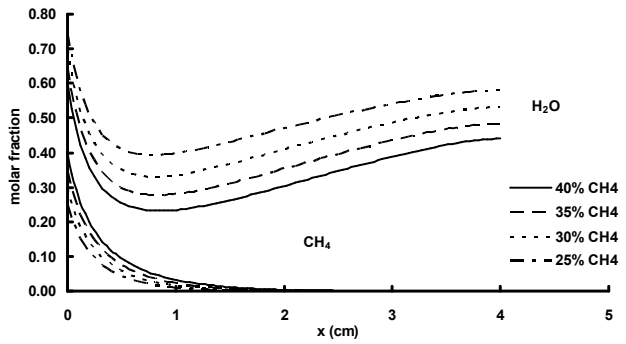

Figure 2: Spatial distribution of CH_4 and H_2O.

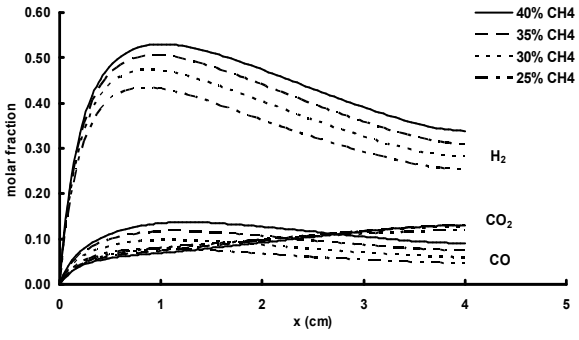

Figure 3: Spatial distribution of H_2, CO and CO_2.

Figure 5 represents the dependence of the current density on the feedstock composition produced for three different values of cell voltage. It is worth mentioning that the percentage of CH_4 in the anodic mixture varies under the assumption of constant mixture moles, in order to keep the volumetric flow-rate constant and, therefore, the energy transport constant, as well. Under this

respect, CH_4 percentage does not directly related to the reforming factor, which usually represents the steam to fuel ratio in the reforming reaction (1), thus, the dependence presented here is not identical to the known reforming factor effect. It is observed that current density increases with CH_4 composition for every cell voltage, since the production of H_2 and CO increases with CH_4 and consequently, the open circuit voltage, *emf* , increases as well. For constant cell voltage, increasing *emf* corresponds to higher overpotential values ($\eta = emf - V_c$) and thus to increased current density. The simulation results seem to follow a practically linear fit, which actually corresponds to the relationship between % mol CH_4 and I, thus the slope of this line represents a quantitative indicator of the cell's efficiency. Additionally, for a given composition, decrease in the cell voltage contributes positively in terms of current density due to the increased overpotential. It can be also seen that current density increases as methane to steam ratio increases towards the thermodynamic limits of solid carbon deposition on the electrode.

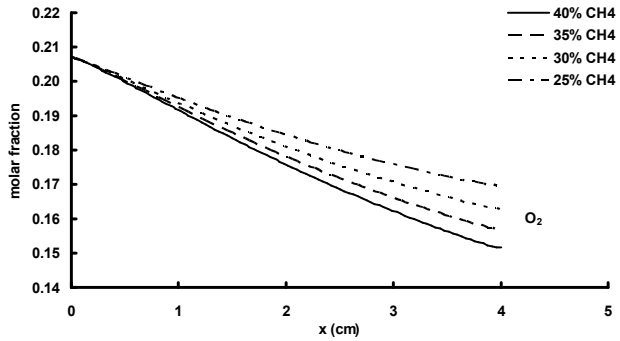

Figure 4: Spatial distribution of O_2.

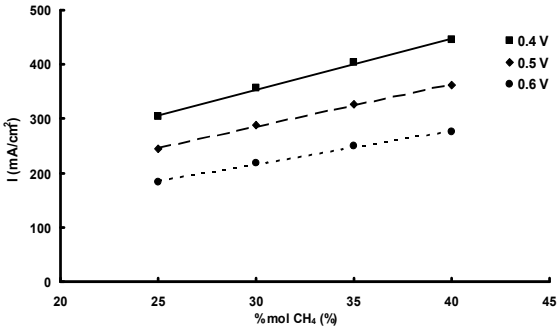

Figure 5: Spatial distribution of CH_4 and H_2O.

Conclusions

This work investigates the relationship between the current density of a typical SOFC with the concentration of CH_4 in the feedstream. The detailed steady-state transport processes have been mathematically described through the relative differential equations along with the appropriate boundary conditions. The above model has been numerically integrated by using the commercially available software CFD-ACE+, and it is found that found that current density increases with the methane concentration in the fuel supply.

References

[1] J.S. Newman and C.W. Tabias:. J. Electrochem. Soc. Vol. 109 (1962), p. 1183.
[2] V. Gurau, H. Liu and S. Kakac: AIChE J. Vol. 44 (1998), p. 2410.
[3] F. Jaouen, G. Lindbergh and G. Sundholm: J. Electrochem. Soc. Vol. 149 (2002), p. A437.
[4] F.A. Coutelieris, S. Douvartzides and P. Tsiakaras: J. Power Sources Vol. 123 (2003), p. 200.
[5] S. Douvartzides, F.A. Coutelieris and P.E. Tsiakaras: J. Power Sources Vol. 5084 (2002), p. 1.
[6] E. Vakouftsi, G. Marnellos, C. Athanasiou and F.A. Coutelieris: Defect Diffusion Forum, Vol. 273-276 (2008), p. 87.
[7] E. Achenbach and E. Reinsche: J. Power Sources Vol. 52 (1994), p. 238.
[8] J.-M. Klein, Y. Bultel, M. Pons and P. Ozil: J. Fuel Cell Tech. Vol. 7 (2007), p. 425.
[9] A.M. Sukeshini, B. Habibzadeh, B.P. Becker, C.A. Stoltz, B.W.Eichhorn and G.S. Jackson: J. Electrochem. Soc. Vol. 154 (2006), p. A705.
[10] P.A. Ramakrishna, S. Yang and C.H. Sohn: J. Power Sources Vol. 158 (2006), p. 378.

Diffusion in Solids and Liquids V
doi:10.4028/www.scientific.net/DDF.297-301

Theoretical Investigation of the Relation between the Output of a Methane Internal Reforming SOFC and the Composition of the Feedstream
doi:10.4028/www.scientific.net/DDF.297-301.838

References

[1] J.S. Newman and C.W. Tabias:. J. Electrochem. Soc. Vol. 109 (1962), p. 1183.
doi:10.1149/1.2425269

[2] V. Gurau, H. Liu and S. Kakac: AIChE J. Vol. 44 (1998), p. 2410.
doi:10.1002/aic.690441109

[3] F. Jaouen, G. Lindbergh and G. Sundholm: J. Electrochem. Soc. Vol. 149 (2002), p. A437.
doi:10.1149/1.1456916

[4] F.A. Coutelieris, S. Douvartzides and P. Tsiakaras: J. Power Sources Vol. 123 (2003), p. 200.
doi:10.1016/S0378-7753(03)00559-7

[5] S. Douvartzides, F.A. Coutelieris and P.E. Tsiakaras: J. Power Sources Vol. 5084 (2002), p. 1.

[6] E. Vakouftsi, G. Marnellos, C. Athanasiou and F.A. Coutelieris: Defect Diffusion Forum, Vol. 273-276 (2008), p. 87.
doi:10.4028/www.scientific.net/DDF.273-276.87

[7] E. Achenbach and E. Reinsche: J. Power Sources Vol. 52 (1994), p. 238.
doi:10.1016/0378-7753(94)02146-5

[8] J.-M. Klein, Y. Bultel, M. Pons and P. Ozil: J. Fuel Cell Tech. Vol. 7 (2007), p. 425.
doi:10.1115/1.2759504

[9] A.M. Sukeshini, B. Habibzadeh, B.P. Becker, C.A. Stoltz, B.W.Eichhorn and G.S. Jackson: J. Electrochem. Soc. Vol. 154 (2006), p. A705.
doi:10.1149/1.2170577

[10] P.A. Ramakrishna, S. Yang and C.H. Sohn: J. Power Sources Vol. 158 (2006), p. 378.
doi:10.1016/j.jpowsour.2005.10.030